Article

Hydroxyapatite–Magnesium Bioceramics: Synthesis and Mechanical–Chemical Characterization

Elizabeth Refugio-Garcia , Alfredo Emiliano Chávez-Pantiga , Gerardo Vázquez-Huerta , José Guadalupe Miranda-Hernández , Carlos Adrián Calles-Arriaga , José Amparo Rodríguez-García , Enrique Rocha-Rangel *

Posted Date: 30 January 2026

doi: 10.20944/preprints202601.2328.v1

Keywords: hydroxiapatite; bioceramics; magnesium; mechanical properties; corrosion

 doi:10.20944/preprints202601.2328.v1

Article

Hydroxyapatite-Magnesium Bioceramics: Synthesis and Mechanical-Chemical Characterization

Elizabeth Refugio-Garcia [1], Alfredo Emiliano Chávez-Pantiga [1], Gerardo Vázquez-Huerta [1], José Guadalupe Miranda-Hernández [2], Carlos Adrián Calles-Arriaga [3], José Amparo Rodríguez-García [3] and Enrique Rocha-Rangel [3,*]

[1] Materials Department, Universidad Autónoma Metropolitana, Av. San Pablo 180, Col. Reynosa-Tamaulipas, CDMX, 2200, México

[2] Industrial Engineering Department, Centro Universitario UAEM Valle de México, Atizapán de Zaragoza, 54500, México

[3] Research Department, Universidad Politécnica de Victoria, Av. Nuevas Tecnologías 5902, Parque Científico y Tecnológico de Tamaulipas, Cd. Victoria 87138, Tamaulipas, México

* Correspondence: erochar@upv.edu.mx

Abstract

Hydroxyapatite (HA) is widely used in biomedical applications due to its biocompatibility and chemical similarity to the mineral phase of bone; however, its low mechanical strength limits its structural use. In this work, HA ceramics with different Mg additions (0, 0.5, 1, 3, 5, and 10% by weight) were prepared using the powder processing technique. The mixtures were homogenized, conformed and sintered at 1100°C. The incorporation of Mg produced a general increase in mechanical properties compared to pure HA. The best mechanical performance was obtained with the formulation containing 5% Mg by weight, achieving a hardness of 319 HV, a porosity of 12.92% and a fracture toughness of 4.06 MPa·$m^{0.5}$, comparable to those reported for human cortical bone, indicating its potential for applications in moderately loaded bone implants. These results suggest that Mg acts as a reinforcing agent in the ceramic matrix, reducing critical defects, which translates into increased mechanical strength. The polarization resistance results show that the incorporation of low fractions by weight of magnesium (1% Mg) optimizes the electrochemical behavior of the material, while higher increases in its concentration cause a slight deterioration of this property.

Keywords: hydroxiapatite; bioceramics; magnesium; mechanical properties; corrosion

1. Introduction

Hydroxyapatite (HA), $Ca_{10}(PO_4)_6(OH)_2$, is a biomaterial extensively used in biomedical applications due to its excellent biocompatibility, bioactivity and close chemical and structural similarity to the mineral phase of human bone [1–5]. These characteristics enable direct bonding with bone tissue, making HA a reference material for orthopedic and dental implants, coatings and bone substitutes. However, the clinical use of pure HA is limited by its low mechanical strength, poor fracture toughness and inadequate performance under dynamic and cyclic loading conditions, which restrict its application in load-bearing environments [6]. To overcome these limitations, HA-based composites rein-forced with bioinert or bioactive metals and ceramics have been widely investigated. The incorporation of hydroxyapatite into metallic matrices, particularly titanium, has proven effective in reducing elastic modulus mismatch and improving bioactivity, thereby minimizing stress shielding. For example, Ti-μHA composites containing 1-3 wt.% hydroxy-apatite exhibited a reduction in elastic modulus from approximately 130 GPa to ~50 GPa, along with enhanced cellular response [7]. Similarly, Fe-nHA composites have demos-traded biomineralization capability, adequate mechanical properties and controllable degradation rates, making them promising candidates for bone tissue engineering applications [8]. Ceramic and glass-based reinforcements have

 doi:10.20944/preprints202601.2328.v1

also been employed to improve the mechanical and biological performance of HA. Bioactive glass-HA composites have shown enhanced mechanical strength while maintaining suitable cellular biocompatibility [9]. In addition, cerium-doped HA-reinforced glass systems exhibited antibacterial properties and promoted osteoblast adhesion and proliferation [10]. The incorporation of silica has further improved the mechanical behavior of HA, with HA-SiO_2 composites containing 20-40% SiO_2 achieving compressive strengths of approximately 165 MPa and enhanced cell adhesion [11]. Carbon-based reinforcements, such as carbon nanotubes, have expanded the functionality of HA composites by increasing hardness, elastic modulus, antimicrobial activity and electrical conductivity, enabling potential applications in bone stimulation and biomedical sensing [12]. Elemental doping via ionic substitution within the HA crystal lattice represents another effective strategy for tailoring material properties. Metals such as titanium, magnesium, zinc and strontium have been incorporated as dopants or secondary phases to improve both mechanical performance and bio-logical response. These substitutions modify the physicochemical properties of HA, in-crease solubility and enhance interactions with bone cells, thereby promoting osteogenesis and implant integration [13,14]. Additionally, ceramic reinforcements including alu-mina, zirconia, β-tricalcium phosphate and bioglasses contribute to improved hardness, wear resistance and thermal stability, while preserving bioactivity and enabling con-trolled degradation and bone regeneration [15]. Among the various dopants, magnesium has attracted considerable attention due to its essential role in bone mineralization and cellular activity regulation. Partial substitution of calcium with magnesium in HA has been reported to improve mechanical properties, optimize in vivo resorption behavior, and stimulate cell proliferation [16]. Furthermore, Mg^{2+} incorporation reduces crystallinity, alters morphology, increases solubility and enhances osseointegration by promoting osteoblast adhesion and differentiation [17,18]. Magnesium-doped hydroxyapatite has been synthesized using various methods, including chemical precipitation, co-precipitation, hydrothermal processing, sol-gel techniques and advanced manufacturing approaches such as spark plasma sintering and three-dimensional printing [6,19]. These synthesis routes allow control over magnesium incorporation, microstructure and the resulting physicochemical, mechanical and biological properties. Since the synthesis method directly influences biocompatibility and in vivo performance, its optimization is crucial for the development of advanced HA-based biomaterials. In this context, the pre-sent study aims to systematically evaluate magnesium-doped hydroxyapatite, focusing on the influence of magnesium content on its structural, mechanical and electrochemical properties, with the objective of contributing to the design of improved biomaterials for bone regeneration applications.

2. Methodology

The powders used for the preparation of the biomaterials were hydroxyapatite and magnesium (particle size: 5-10 μm, purity: 99.9%, Sigma-Aldrich). The studied chemical compositions are listed in Table 1.

Table 1. Composition of different prepared formulations.

Composition	Magnesium (weight %)	Hydroxyapatite weight %
HA-0%Mg	Mg 0	100
HA-0.5%Mg	Mg 0.5	99.5
HA-1%Mg	Mg 1	99
HA-3%Mg	Mg 3	97
HA-5%Mg	Mg 5	95
HA-10%Mg	Mg 10	90

 doi:10.20944/preprints202601.2328.v1

The initial hydroxyapatite-magnesium powder mixtures were grinded in a ball mill (Lab Mill-8000) at 400 rpm for 9 h. Zirconia milling media with a diameter of 3 mm were used. The milling process was performed under dry conditions, with the addition of 1 mL of isopropyl alcohol as a process control agent. A powder-to-ball weight ratio of 1:20 was employed. The milled powders were subsequently compacted into cylindrical pellets by uniaxial pressing using a hardened steel die under an applied pressure of 200 MPa. The pellets were sintered in an electric furnace (Nabertherm) at 1100 °C with a dwell time of 1 h. The sintering process was conducted under vacuum, using a heating rate of 10 °C/min. After completion of the thermal cycle, the furnace was switched off and the samples were allowed to cool naturally inside the furnace. After sintering, the physical characterization of the composites was performed. The density was determined according to Archimedes' principle, following the ASTM B963 standard [20]. Fracture toughness was evaluated using the indentation fracture method [21], applying the equation proposed by Evans [22]. Microhardness measurements were carried out in accordance with the ASTM E384-16 standard [23]. For this analysis, twelve indentations were performed at different locations on each sample, and the reported values correspond to the average of these measurements. Microhardness tests were conducted using a microhardness tester (Emco-Test, DuraScan 200). The microstructural characteristics of the composites were examined by optical microscopy (Olympus) at a magnification of 20X. Prior to observation, the samples were ground and polished using standard metallographic procedures to obtain a flat and reflective surface. For the degradation resistance assessment, the samples were immersed in a physiological solution with an isotonic composition of 0.9% sodium chloride (NaCl) for 30 min prior to testing in order to ensure surface saturation. Electrochemical measurements were carried out using a potentiostat-galvanostat (Zahner Zennium) in a conventional three-electrode cell configuration. The HA–Mg composites served as the working electrodes (WE), an Ag/AgCl electrode in 3 M NaCl was used as the reference electrode (RE), and a graphite rod acted as the counter electrode (CE). Electrochemical impedance spectroscopy (EIS) was employed to evaluate the polarization resistance (Rp), providing insight into the degradation behavior of the samples. The EIS measurements were per-formed by applying a sinusoidal perturbation of ±10 mV over a frequency range from 100 kHz to 100 mHz. Prior to each measurement, the system was allowed to reach a stable open-circuit potential. For each composition, two impedance spectra were recorded, and the resulting Nyquist plots were extrapolated to obtain complete semicircles, from which the corresponding Rp values were determined.

3. Results

3.1. Density and Porosity

Figure 1 presents the relative density and porosity of the sintered ceramics as a function of magnesium content. An inverse relationship is observed, with increasing magnesium content leading to a decrease in relative density and a corresponding increase in porosity, indicating a reduction in densification during sintering. Although high density is typically associated with improved mechanical properties, a certain degree of porosity is required for biomedical applications to promote biointegration. Cortical bone exhibits porosity values of approximately 15% [24], which are slightly higher than those obtained for ceramics containing 3, 5, and 10% magnesium. This similarity suggests that the developed ceramics possess porosity levels compatible with bone tissue, potentially favoring bone ingrowth and reducing stress-shielding effects. Therefore, despite the decrease in relative density with increasing magnesium content, the resulting porosity particularly at lower magnesium concentrations is considered suitable for the intended biomedical application.

 doi:10.20944/preprints202601.2328.v1

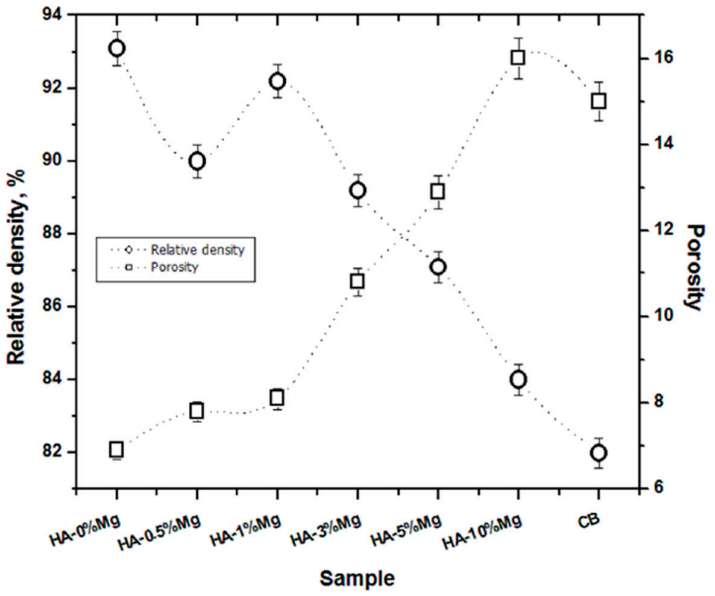

Figure 1. Relative density and porosity values obtained for each sintered ceramic. CB – cortical bone [24].

3.2. Microstructure

Figure 2 shows the microstructures of the hydroxyapatite–magnesium ceramics observed by optical microscopy at 20X magnification. The pure hydroxyapatite sample (Figure 2a) exhibits a homogeneous ceramic matrix, consistent with its higher relative density and lower porosity reported in Figure 1. Upon the addition of 0.5 wt% Mg (Figure 2b), the metallic phase appears as fine, bright particles uniformly dispersed within the hydroxyapatite matrix, which correlates with the slight decrease in relative density and the moderate increase in porosity observed at this magnesium content. For samples containing 1, 3, and 5 wt% Mg (Figures 2c-e), a generally homogeneous microstructure is still observed; however, the magnesium-rich particles become fewer in number and larger in size compared to the 0.5 wt% Mg sample. This particle coarsening and partial agglomeration are consistent with the progressive reduction in densification and the corresponding increase in porosity reported in Figure 1, suggesting that higher magnesium contents increasingly hinder mass transport during sintering. In contrast, the sample containing 10 wt% Mg (Figure 2f) exhibits larger and irregular bright regions, indicative of magnesium-rich segregation zones. This microstructural heterogeneity agrees with the lowest relative density and highest porosity values measured for this composition, confirming that excessive magnesium content promotes non-uniform densification and pore retention. No significant porosity is directly observed in the optical micrographs, indicating that the pores are likely below the resolution limit of optical microscopy. Nevertheless, the porosity quantified in Figure 1 is likely associated with fine and uniformly distributed pores within the ceramic matrix. Additionally, based on the scale reference and the absence of clearly defined grain boundaries, the average grain size is inferred to be below 1 μm, which may also contribute to the observed densification behavior.

 doi:10.20944/preprints202601.2328.v1

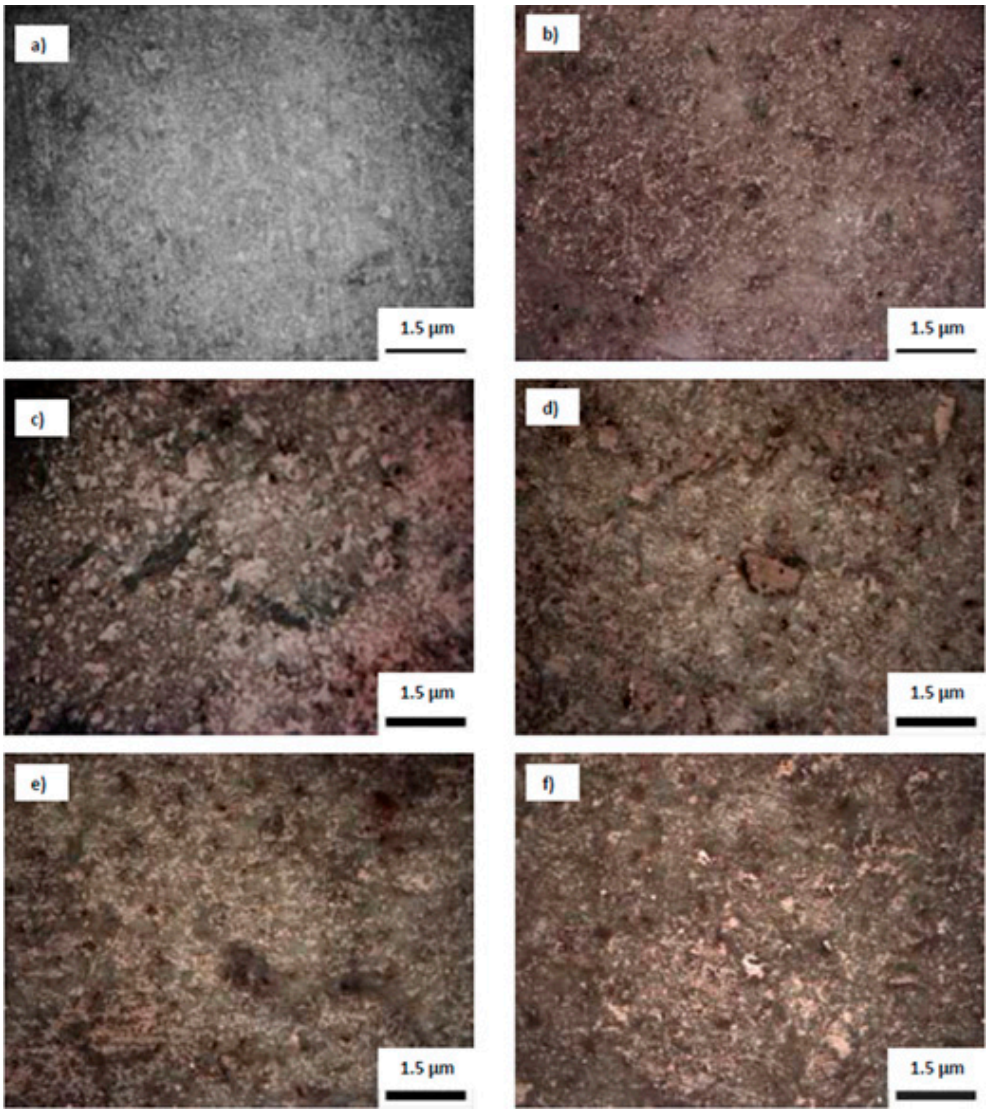

Figure 2. Microstructures of the different Hydroxyapatite–Magnesium ceramics obtained by optical microscopy at 20X magnification. a) HA-0%Mg b) HA-0.5%Mg c) HA-1%Mg d) HA-3%Mg e) HA-5%Mg f) HA-10%Mg.

3.3. Microhardness and Fracture Toughness

Figure 3 shows the microhardness values of the hydroxyapatite–magnesium ceramics. A progressive decrease in microhardness is observed with increasing magnesium content, which is consistent with the reduction in relative density and the increase in porosity reported in Figure 1, as well as with the microstructural changes observed in Figure 2. At low magnesium contents (0.5-1 wt%), microhardness values decrease significantly, approaching those of cortical bone. This behavior can be attributed to the homogeneous dispersion of magnesium-rich particles and the moderate porosity developed at these compositions, which may improve mechanical compatibility with natural bone. In contrast, higher magnesium contents (≥3 wt%) result in a pronounced reduction in microhardness, correlating with increased porosity and microstructural heterogeneity. For reference, the microhardness value reported in the literature for pure hydroxyapatite is included in figure 3 and is significantly higher than those measured in the ceramics developed in this study, highlighting the effect of magnesium addition on tailoring the mechanical response.

 doi:10.20944/preprints202601.2328.v1

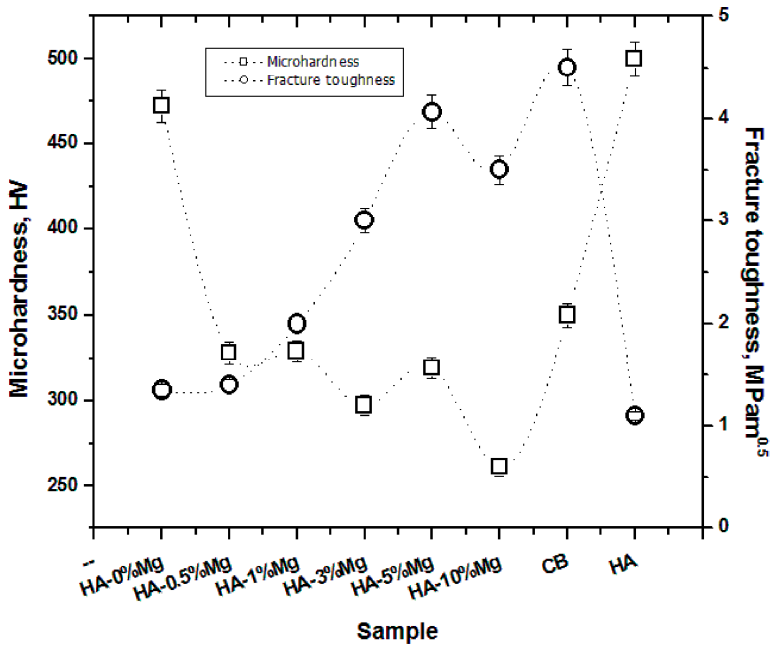

Figure 3. Microhardness and fracture toughness values obtained for each sintered ceramic. CB – cortical bone [25], HA [3].

Figure 3 also presents the fracture toughness of hydroxyapatite with different magnesium contents, together with reference values for cortical bone and pure HA. An increase in fracture toughness is observed with increasing magnesium content up to 5 wt% Mg, followed by a decrease at 10 wt% Mg. Despite this reduction, the toughness at 10 wt% Mg remains higher than that of pure HA and low-magnesium compositions. This behavior indicates the existence of an optimal magnesium content, in the range of 3-5 wt%, for enhancing fracture resistance. The improvement in fracture toughness at intermediate magnesium contents is consistent with the microstructural features discussed in Figure 2 and the densification behavior reported in Figure 1. The homogeneous dispersion of magnesium-rich particles and the moderate porosity observed up to 5 wt% Mg may promote energy dissipation mechanisms, such as crack deflection and microcrack formation, thereby enhancing toughness. In contrast, the decrease in toughness at 10 wt% Mg correlates with increased porosity and microstructural heterogeneity, including magnesium-rich segregation zones, which may act as preferential crack initiation sites. When these results are considered together with the microhardness data, an inverse trend between hardness and toughness is observed. While increasing magnesium content reduces microhardness due to lower relative density and possible formation of less rigid phases, it simultaneously enhances fracture toughness by promoting more damage-tolerant microstructures. Cortical bone exhibits a similar combination of moderate hardness and relatively high toughness. In this regard, ceramics containing 3-5 wt% Mg show mechanical properties closest to those of cortical bone, achieving a compromise between hardness reduction and toughness enhancement. These results indicate that magnesium acts as an effective reinforcing and toughening agent in hydroxyapatite. A magnesium content of approximately 3–5 wt% appears to be optimal for biomedical applications requiring mechanical compatibility with bone and enhanced fracture resistance.

3.4. Electrochemical Impedance Spectroscopy

Figure 4 presents the Nyquist plots obtained for the HA–Mg composites and bovine bone immersed in a physiological solution of 0.9% NaCl. In all cases, the impedance spectra exhibit

 doi:10.20944/preprints202601.2328.v1

depressed and incomplete semicircles, which were extrapolated to determine their intersection with the real impedance axis (Z_real). The diameter of each semicircle corresponds to the polarization resistance (Rp), whose values are summarized in Figure 5. The impedance response does not show a linear dependence on magnesium content. The sample containing 1 wt% Mg exhibits the highest impedance and, consequently, the highest Rp value, indicating superior corrosion resistance among the studied compositions. Samples with 3 and 5 wt% Mg also present relatively high impedance values, although lower than those observed for 1 wt% Mg. In contrast, pure hydroxyapatite and bovine bone show the lowest impedance values, suggesting lower resistance to ionic transport and a higher susceptibility to degradation under physiological conditions. The samples containing 0.5 and 10 wt% Mg exhibit intermediate behavior. This non-monotonic trend is consistent with the microstructural and porosity results discussed in Figures 1 and 2. At low to intermediate magnesium contents, particularly around 1 wt%, the homogeneous dispersion of magnesium-rich phases and the moderate porosity may favor the formation of a more stable and protective surface layer, limiting ionic penetration and improving corrosion resistance. Conversely, higher magnesium contents, such as 10 wt%, are associated with increased porosity and microstructural heterogeneity, including segregation zones, which may act as preferential pathways for electrolyte infiltration and reduce the overall polarization resistance.

When considered alongside the mechanical results, these electrochemical findings further highlight the role of magnesium as a multifunctional modifier of hydroxyapatite. While intermediate magnesium contents (3-5 wt%) optimize fracture toughness and mechanical similarity to cortical bone, lower magnesium additions (~1 wt%) provide superior electrochemical stability. This indicates that the optimal magnesium content depends on the targeted balance between mechanical performance and corrosion resistance. From all these it is possible to conclude that the electrochemical behavior of the HA–Mg composites is strongly governed by their microstructural characteristics and porosity, reinforcing the conclusion that controlled magnesium addition is an effective strategy to tailor both the mechanical and degradation behavior of hydroxyapatite-based biomaterials.

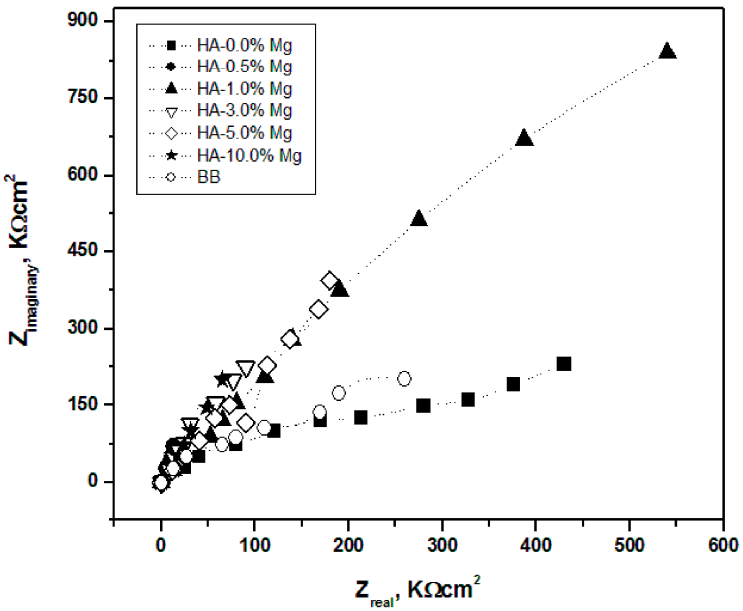

Figure 4. impedances of hydroxyapatite (HA) samples with different magnesium contents. BB - bovine bone.

 doi:10.20944/preprints202601.2328.v1

Figure 5 shows the variation in polarization resistance (Rp) of hydroxyapatite with different magnesium contents, together with bovine bone. A significant increase in Rp is observed at low magnesium contents, with the HA-1 wt% Mg sample exhibiting the highest value (551 kΩ·cm²), exceeding pure HA (443 kΩ·cm²) and bovine bone (274 kΩ·cm²). This improvement is consistent with the impedance results (Figure 4) and correlates with the homogeneous microstructure and moderate porosity observed at low magnesium contents (figures 1 and 2). In contrast, magnesium contents above 3 wt% result in a marked decrease in Rp, reaching 182 kΩ·cm² at 3 wt% Mg and 73 kΩ·cm² at 10 wt% Mg. This deterioration agrees with the increased porosity, reduced relative density, and microstructural heterogeneity reported at higher magnesium levels, which may facilitate electrolyte penetration and corrosion. When considered alongside the mechanical results, these findings reveal a trade-off between electrochemical stability and mechanical performance. While intermediate magnesium contents (3-5 wt%) enhance fracture toughness and mechanical similarity to cortical bone, low magnesium addition (~1 wt%) provides superior corrosion resistance. Therefore, it can be remarked that magnesium content is a key parameter for adapting the functional behavior of HA-based ceramics for biomedical applications.

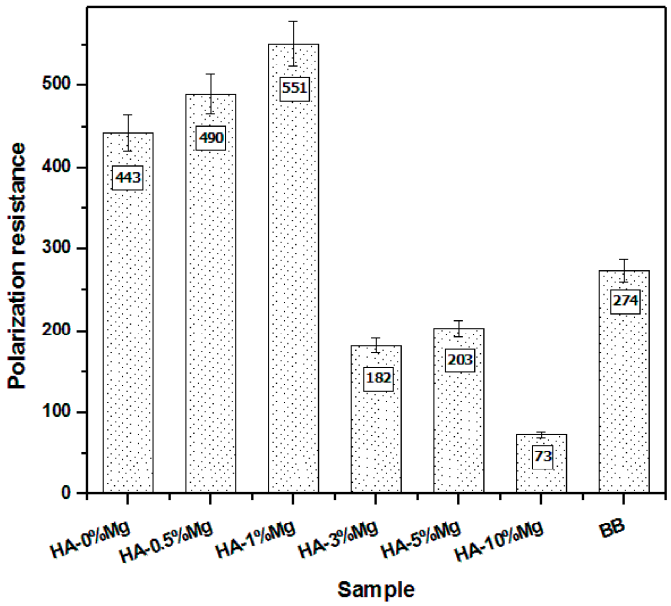

Figure 5. Polarization resistance (Rp) of hydroxyapatite (HA) samples with different magnesium contents. BB – bovine bone[26].

5. Conclusions

- The controlled incorporation of magnesium into hydroxyapatite by powder-processing techniques effectively tailored the microstructural, mechanical, and electrochemical properties of the ceramics. Magnesium addition influenced densification and porosity, producing homogeneous microstructures at low to intermediate contents, which directly impacted the functional performance of the materials.
- From a mechanical perspective, magnesium contents of 3-5 wt% provided a favorable balance between reduced microhardness and enhanced fracture toughness, resulting in properties close to those of cortical bone. In contrast, higher magnesium contents promoted microstructural heterogeneity and increased porosity, negatively affecting mechanical performance.
- Electrochemical results showed that low magnesium incorporation significantly im-proved corrosion resistance. The HA-1 wt% Mg composition exhibited the highest polar-ization

 doi:10.20944/preprints202601.2328.v1

resistance (551 kΩ·cm²), exceeding that of pure hydroxyapatite and bovine bone, while higher magnesium contents led to reduced electrochemical stability.

- Overall, these findings demonstrate that controlled magnesium doping enables the optimization of both mechanical and electrochemical behavior in hydroxyapatite-based ceramics, supporting their potential use as biomaterials for medical applications.

Author Contributions: Conceptualization, M.E.R.-G and E.R.-R; methodology, A.E.C.-P, M.E.R.-G., G.V.-H. and J.G.M.-H.; software, J.A.R.-G.; validation, A.E.C.-P, M.E.R.-G., G.V.-H. and J.G.M.-H.; formal analysis, M.E.R.-G and E.R.-R; investigation, A.E.C.-P, M.E.R.-G., G.V.-H. and J.G.M.-H.; resources, M.E.R.-G and E.R.-R; data curation, C.A.C.-A. and J.A.R.-G.; writing—original draft preparation, A.E.C.-P, M.E.R.-G., G.V.-H. and E.R.-R; writing—review and editing, C.A.C.-A. and J.A.R.-G.; visualization, M.E.R.-G, G.V.-H. and E.R.-R; supervision, M.E.R.-G and E.R.-R; project administration, M.E.R.-G, G.V.-H. and E.R.-R; funding acquisition, M.E.R.-G and E.R.-R. All authors have read and agreed to the published version of the manuscript.

Funding: This research received no external funding.

Data Availability Statement: The original contributions presented in this study are included in the article. Further inquiries can be directed to the corresponding author.

Acknowledgments: The authors would like to thank UAM, UAEM and UPV for the support provided in the use of their facilities during the development of this work.

Conflicts of Interest: The authors declare no conflicts of interest.

Abbreviations

The following abbreviations are used in this manuscript:

HA	Hydroxyapatite
CB	Cortical bone
BB	Bovine bone
HV	Hardness Vickers
SPS	Spark plasma sintering
CE	Counter electrode
EIS	Electrochemical impedance spectroscopy
Rp	Polarization resistance
wt	Weight

References

1. Shi, H.; Zhou, Z.; Li, W.; Fan, Y.; Li, Z.; Wei, J. Hydroxyapatite based materials for bone tissue engineering: A brief and comprehensive introduction. *Crystals* **2021**, 11, 149. https://doi.org/10.3390/cryst11020149
2. Fendi, F.; Abdullah, B.; Suryani, S.; Usman, A.N.; Tahir, D. Development and application of hydroxyapatite-based scaffolds for bone tissue regeneration: A systematic literature review. *Bone* **2024**, 183, 117075. https://doi.org/10.1016/j.bone.2024.117075
3. Fiume, E.; Magnaterra, G.; Rahdar, A.; Verné, E.; Baino, F. Hydroxyapatite for biomedical applications: A short overview. Ceramics **2021**, 4, 542–563. https://doi.org/10.3390/ceramics4040039
4. Lin, K.; Chang, J. Structure and properties of hydroxyapatite for biomedical applications. In Hydroxyapatite (HAp) for Biomedical Applications; Mucalo, M., Ed.; Woodhead Publishing: Cambridge, UK, **2015**; pp. 3–19. https://doi.org/10.1016/B978-1-78242-033-0.00001-8
5. Szcześ, A.; Hołysz, L.; Chibowski, E. Synthesis of hydroxyapatite for biomedical applications. *Adv. Colloid Interface Sci.* **2017**, 249, 321–330. https://doi.org/10.1016/j.cis.2017.04.007
6. Dorozhkin, S.V. Bioceramics of calcium orthophosphates. *Biomaterials* **2010**, 31, 1465–1485. https://doi.org/10.1016/j.biomaterials.2009.11.050
7. Topuz, M.; Dikici, B.; Gavgali, M. Titanium-based composite scaffolds reinforced with hydroxyapatite-zirconia: Production, mechanical and in-vitro characterization. *J. Mech. Behav. Biomed. Mater.* 2021, 118, 104480. https://doi.org/10.1016/j.jmbbm.2021.104480

 doi:10.20944/preprints202601.2328.v1

8. Rabeeh, V.P.M.; Surendramohan, K.S.; Jyothis, S.; Rahim, S.A.; Babu, C.S.; Sijina, K.P.; Rajanikant, G.K.; Joseph, M.A.; Hanas, T. Fostering biomineralization and biodegradation: nano-hydroxyapatite reinforced iron composites for biodegradable implant application. *Discover Materials*. **2024**, 4, 39. https://doi.org/10.1007/s43939-024-00113-6
9. Meechoowas, E.; Naknikham, U.; Tungsanguan, O.; Martvijit, S.; Pamok, C.; Tapasa, K. Development and characterization of bioactive glass: Preliminary study for medical applications. *Mat Tod. Proc*, **2022**, 65, 2407-2411. https://doi.org/10.1016/j.matpr.2022.05.528
10. Ciobanu, C.S.; Iconaru, Popa, C.L.; Motelica-Heino, M.; Predoi, D. Evaluation of Samarium Doped Hydroxyapatite, Ceramics for Medical Application: Antimicrobial Activity. *J. Nanomats*. **2015**, 849216, http://dx.doi.org/10.1155/2015/849216
11. Patel, P.; Buckley, C.; Taylor, B.; Sahyoun, C.C.; Patel, S.D.; Mont, A.J.; Mai, L.D.; Patel, S.; Freeman, J.W. Mechanical and biological evaluation of a hydroxyapatite-reinforced scaffold for bone regeneration. *J. Biomed. Mater. Res. Part A.* **2019**, 107, 732-741. http://dx.doi.org/*10.1002/jbm.a.36588*.
12. White, A.A.; Best S.M.; Kinloch, I. Hydroxyapatite–Carbon Nanotube Composites for Biomedical Applications: A Review. *Int. J. Appl. Ceram. Technol.* **2007**, 4, 1 – 13. http://dx.doi.org/10.1111/j.1744-7402.2007.02113.x.
13. Boanini, E.; Gazzano, M.; Bigi, A. Ionic substitution in calcium phosphates synthesized at low temperature. *Acta Biomater*. **2010**, 6, 1882–1894. https://doi.org/10.1016/j.actbio.2009.12.041
14. Bose, S.; Tarafder, S. Calcium phosphate ceramic systems in growth factor and drug delivery for bone tissue engineering: A review. *Acta Biomater*. *2012*, 8, 1401–1421. https://doi.org/10.1016/j.actbio.2011.11.017
15. Liu, D.M.; Troczynski, T.; Tseng, W.J. Water-based sol–gel synthesis of hydroxyapatite: Process development. *Biomaterials* **2001**, 22, 1721–1730. https://doi.org/10.1016/S0142-9612(00)00332-X
16. Kanasan, N.; Adzila, S.; Koh, C.T.; Rahman, H.A.; Panerselvan, G. Effects of magnesium doping on the properties of hydroxyapatite/sodium alginate biocomposite. *Adv Appl Ceram.* **2019**, 118, 1-6. https://doi.org/10.1080/17436753.2019.1611983
17. Zhang, A.-M.; et al. Advances in hydroxyapatite coatings on biodegradable magnesium and its alloys. *J. Magnes. Alloys* **2022**, 10, 1154–1170. https://doi.org/10.1016/j.jma.2022.01.001
18. Bigi, A.; Falini, G.; Foresti, E.; Ripamonti, A.; Gazzano, M.; N. Roveri. Magnesium influence on hydroxyapatite crystallization. *J. Inorg. Biochem*. **1993**, 49, 69–78. https://doi.org/10.1016/0162-0134(93)80049-F
19. Hassan, M.N.; Mahmoud, M.M.; Link, G.; El-Fattah, A.A.; Kandil, S. Sintering of naturally derived hydroxyapatite using high frequency microwave processing. *J. Alloys Compd.* **2016**, 682, 107–114. https://doi.org/10.1016/j.jallcom.2016.04.266
20. ASTM B962-15. Standard Test Methods for Density of Compacted or Sintered Powder Metallurgy (PM) Products Using Archimedes' Principle; ASTM International: West Conshohocken, PA, USA, **2015**.
21. Rocha-Rangel, E. Fracture Toughness Determinations by Means of Indentation Fracture. In Nanocomposites with Unique Properties and Applications in Medicine and Industry; John, C., Ed.; IntechOpen: London, UK, **2011**; pp. 1–18. https://doi.org/10.5772/18127
22. Evans, A.G.; Charles, E.A. Fracture Toughness Determination by Indentation. *J. Am. Ceram. Soc*. **1976**, 59, 371–372. http://dx.doi.org/10.1111/j.1151-2916.1976.tb10991.x
23. ASTM E384-16. Standard Test Method for Microindentation Hardness of Materials; ASTM International: West Conshohocken, PA, USA, **2016**.
24. Jerban, S.; Ma, Y.; Wan, L.; Searleman, A.C.; Jang, H.; Sah, R.L.; Chang, E.Y.; Du, J. Collagen proton fraction from ultrashort echo time magnetization transfer (UTE-MT) MRI modelling correlates significantly with cortical bone porosity measured with micro-computed tomography (μCT). *NMR Biomed*. **2019**, 32, e4099. https://doi.org/10.1002/nbm.4045

 doi:10.20944/preprints202601.2328.v1

25. Mirzaali, M.J.; Schwiedrzik, J.J.; Thaiwichai, S.; Best, J.P.; Michler, J.; Zysset, P.K.; Wolframa, U. Mechanical properties of cortical bone and their relationships with age, gender, composition and microindentation properties in the elderly. *Bone* **2016**, 93, 196–211. https://doi.org/10.1016/j.bone.2015.11.018
26. Vargas-Coronado, R.F.; Chan-Chan, L.H.; Cervantes-Uc, J.M.; Cauich-Rodríguez, J.V.; Piña Barb. M.C. Characterization of Bone Cements Prepared with either Hydroxyapatite, α-TCP or Bovine Bone. *Rev. Mex. Ing. Biomed*. **2013**, 34, 89–96.